BEAM-BEAM EFFECTS WITH STRONG BETATRON COUPLING AT INTERACTION POINT

S.A. Nikitin and E.A. Simonov* BINP SB RAS, Novosibirsk, 630090, Russia

Abstract

Study of the solenoid compensation scheme at VEPP-4M collider, based on the use of two skew quads, has been performed in the viewpoint of beam-beam (b.-b.) effects. Simulation and experimental results are presented and dicussed.

1 INTRODUCTION

To compensate a betatron coupling arised in a storage ring because of the longitudinal magnetic field of a particle detector the anti-solenoids are mainly applied. An alternative way is the use of special skew quads instead of or in combination with anti-solenoids. Application of such kind compensation schemes may be of interest in the viewpoint of an additional control of beam parameters affecting the luminosity. For example, three pairs of quadrupole lenses rotated through different angles serve for this aim at CESR [1]. Some versions to compensate the influence of the KEDR detector field on betatron coupling at the VEPP-4M collider were considered in [2] based on a very simple scheme with two skew quads (TSQ) proposed by Steffen for PETRA [3]. Normally, the KEDR solenoid compensation will be performed with the use of two superconducting anti-solenoids. In the alternative case, the coupling is localized at the section including KEDR in the center and ended by a skew quad at both sides. As was shown [2] for this case, the aspect ratio, namely, the ratio of vertical beam size σ_Z^* to horizontal one σ_X^* at the interaction point (IP), can be considerably increased depending on the longitudinal field magnitude H. On the face of it, it enables to increase a luminosity owing to increasing the current I of colliding beams. But, since $\sigma_X^* \approx const$, one can increase I till the radial b.-b. parameter $\xi_X \propto I\beta_X^*/(\sigma_X^*)^2$ reaches a critical level (it is assumed that, as usually, $\xi_X < \xi_Z \propto I\beta_Z^*/(\sigma_Z^*\sigma_X^*)$). Besides, a role of strong betatron coupling at IP as well as an influence of large radial dispersion at IP are not clear a priori. To clarify main limitations we have performed some appropriate machine study experiments and b.-b. simulations. Note, other known methods to enlarge beam sizes with the aim to increase a luminosity by storing more the beam current differ from the TSQ method in principle features. The method based on excitation of betatron coupling resonance makes the betatron tunes mutually dependent that hampers tuning of the work point. The use of strong wiggler magnets for "beam blow up" gives a significant increase of energy spread that may be undesirable in some high energy physics experiments, especially with narrow resonances.

* E.A.Simonov@inp.nsk.su

2 TSQ SCHEME AT VEPP-4M

The skew quads are placed symmetrically regarding to IP at "magic" azimuths determined by the special equation for the focucing parameters [2, 3]. Their strengths must be equal in absolute value and opposite in sign; the magnitude of strength is found from the relation with the longitudinal field magnitude. Satisfaction of all these conditions eliminates a split of betatron frequencies caused by the longitudinal magnetic field. The 4x4 matrix of the betatron phase space transformation at one turn does not contain adiagonal blocks for the azimuths beyond the coupling localization section. Inside this section, including IP, the elements of adiagonal blocks become significant. At the ends of the VEPP-4M mini-beta insert there are two standard skew quadrupole correctors 20 cm in length which are just close in position to the "magic" azimuths. The use of these correctors enables an experimental study of the TSQ method without any alteration in the magnetic structure. During the run of 2000 year when the field of the superconducting KEDR magnet was turned on up to a nominal level of $H \sim 0.5$ Tesla with a zero field of antisolenoids we tested the TSQ scheme ($E = 1.5$ GeV). A quality of betatron coupling localization may be characterized by a residual width of the coupling resonance ($\Delta\nu_C$) and an amplitude of vertical dispersion function η_Z. For all values of H from an interval under study from 0 to 0.5 Tesla $\Delta\nu_C \leq 5 \cdot 10^{-3}$, $|\eta_Z| << |\eta_X|$ where η_X is a radial dispersion function (in the case without any compensation $\Delta\nu_C$ exceeds 0.05 at $H = 0.3$ Tesla, $|\eta_Z| \sim |\eta_X|$). In Fig.1 the calculated and measured dependences of the vertical beam size at IP upon the field H are presented. The size σ_Z^* was determined
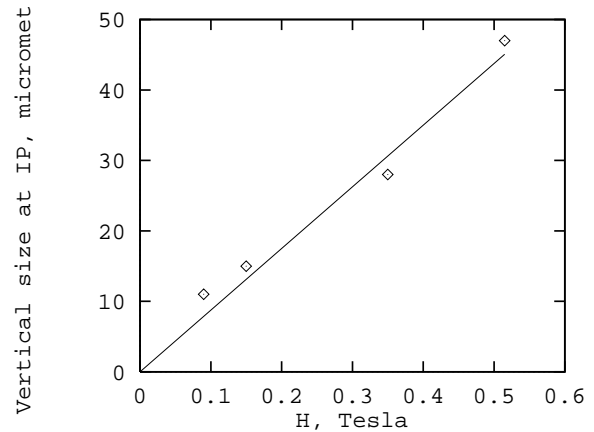

Figure 1: The vertical beam size at IP calculated (the solid line) and measured by a specific luminosity (rhombs) vs. the KEDR field for the TSQ case ($E = 1.5$ GeV).

from the measured specific luminosity ($\sigma_X^* \approx const$). In the case of conventional solenoid compensation (or of zero field H) the natural vertical size σ_Z^* is about of 5 μm at the coupling coefficient (a ratio of the vertical emittance to the radial one) of $\sim 10^{-2}$. So the use of TSQ increases the aspect ratio in 10 times at $H \sim 0.5$ Tesla.

3 BEAM-BEAM SIMULATION MODEL

The simulation ultra-relativistic model is based on the weak-strong approximation with taking into account for the longitudinal motion. The weak beam consists of some probe particles which execute a 6D motion and interact with the steady strong beam. The strong beam is represented as a thick nonlinear lens with the Gauss distribution of density in all three dimensions. The betatron and the synchrotron motion of the probe particles along the ring are described in linear approximation with the help of the symplectic matrices. Total transformation of betatron coordinates at one turn is added by a transformation accounting for radiation damping and quantum excitation. To calculate a probe particle motion through IP the following known algorithms are used [4]:

- Disruption. The strong beam is divided by some slices along the longitudinal direction. The transverse coordinates of a probe particle vary while it moves from one slice to another; the particle momentum is changed at intersection of the slices.
- HourGlass Effect. Transverse sizes of the strong beam (i.e. of separate slices) depend upon the azimuth of interaction between the probe particle and the slice.
- The variation of the transverse particle momentum is described by the Bassetti-Erskine formula. The longitudinal momentum is changed in accordance with the Hirata formula which conserves the symplecticity.

The simulation code for the ensemble of ten probe particles takes statistics during hundreds of the damping time and computes the vertical size of the weak beam depending on the b.-b. parameter and the detector magnetic field.

4 SIMULATION AND EXPERIMENTAL RESULTS

The Fig.2-7 demonstrate the results of simulation for the case of TSQ compensation at various values of H and of the radial dispersion function η_X^* at IP ($E = 1.5$ GeV). For VEPP-4M $\eta_X^* = 80$. The case $\eta_X^* = 0$ is a model situation. The b.-b. parameter is determined as

$$\xi_Z = \frac{N r_0 \beta_Z^*}{2\pi\gamma\sigma_Z^*(\sigma_Z^* + \sigma_X^*)}$$

where σ_Z^* and σ_X^* are assumed, here and further, to be sizes not disturbed by b.-b. effects. Two calculated values are under comparison: the vertical beam size at IP and one at the technical section with RF system. The size at RF grows more faster with ξ_Z than the size at IP. This tendency
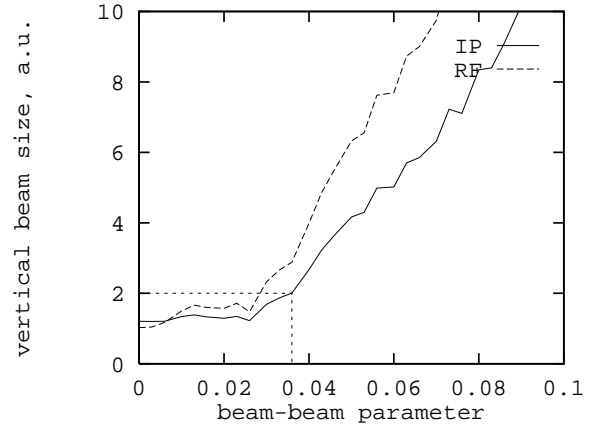

Figure 2: The simulated vertical beam size at IP (the solid line) and at the RF system (the dashed line) normalized to their values not disturbed by b.-b. effects versus ξ_Z at $H = 0.06$ Tesla, $\eta_X^* = 80$ cm.
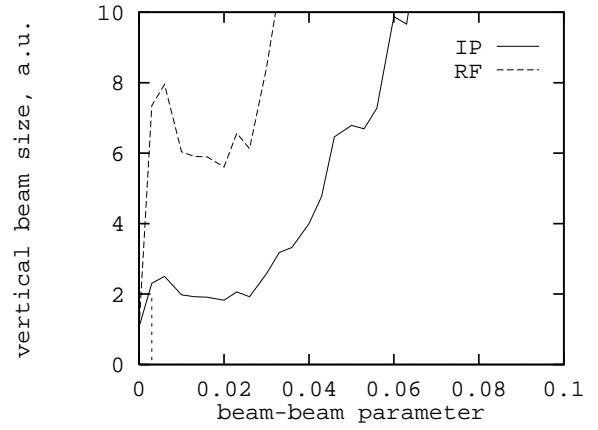

Figure 3: $H = 0.14$ Tesla, $\eta_X^* = 80$ cm.

is sustained by a simple model of linear lens placed at IP. Explanation is a significant initial size at IP. Let ξ_C be a critical value of the b.-b. parameter, which is determined as shown in Fig.2-7 by a criterion of doubling in size at IP. The typically attainable luminosity may be estimated as:

$$L_t = \frac{\pi\gamma^2 \xi_C^2 \sigma_Z^* (\sigma_X^* + \sigma_Z^*)^2 f_0}{(r_e \beta_Z^*)^2 \sigma_X^*}.$$

Simulated and measured behaviors of L_t for VEPP-4M depending upon the field H are represented in Fig.8. Collapses of the calculated curve between values $H = 0.1$ and $H = 0.2$ as well as above $H = 0.25$ Tesla correlate with experiment. An advantage of the TSQ method ("1") over usual ones ("2") may be possible only in those ranges of H where $(\xi_C^2 \sigma_Z^*)_1/(\xi_C^2 \sigma_Z^*)_2 > 1$. In the case $\eta_X^* = 80$ cm, because of a significant decrease of ξ_C (from ~ 0.045 to ~ 0.025 - see Fig.2-4), such a condition is not realized sufficiently. Maximal luminosity of $\sim 3 \cdot 10^{29}$ does not exceed the level of $5 \cdot 10^{29}$ achieved in a whole series of experiments with $H = 0$ at E=1.5 GeV. In the model case $\eta_X^* = 0$, the parameter ξ_C drops by 10% only (see
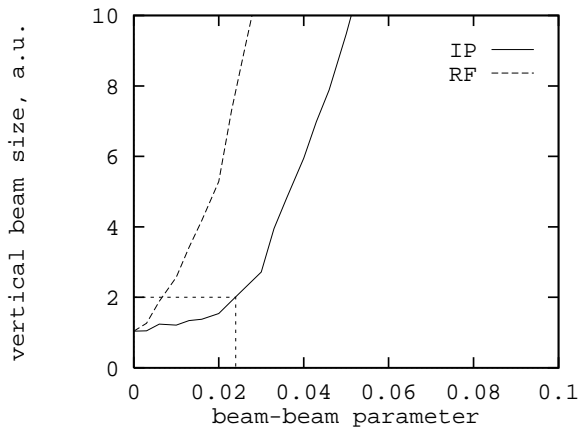
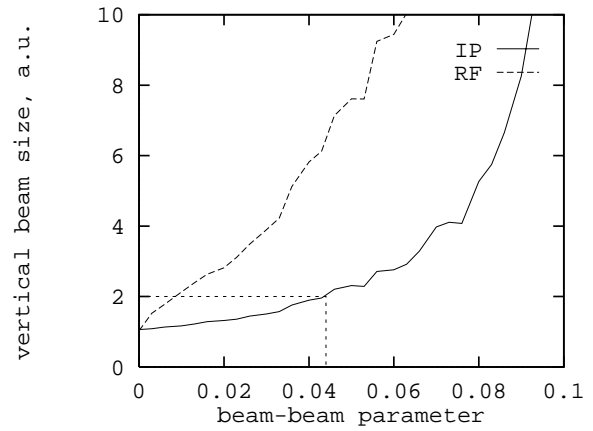Figure 4: $H = 0.18$ Tesla, $\eta_X^* = 80$ cm.

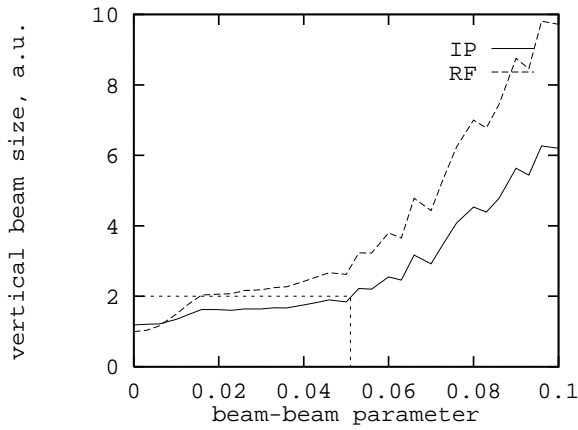Figure 5: $H = 0.06$ Tesla, $\eta_X^* = 0$.

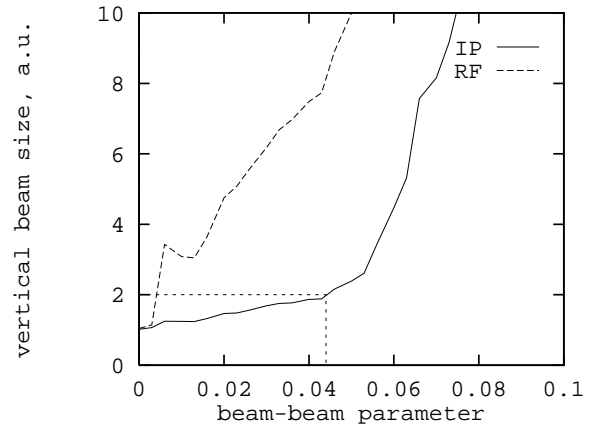

Figure 6: $H = 0.14$ Tesla, $\eta_X^* = 0$.

Figure 7: $H = 0.18$ Tesla, $\eta_X^* = 0$.

Fig.5-7) and so the use of TSQ holds good promise. Generally, to optimize the aspect ratio retaining the detector field magnitude one can combine in the TSQ scheme both two skew quads and anti-solenoids (proved by calculations for VEPP-4M). Then the parameter H equals to an effective field determined through a noncompensated part of a detector field integral.

5 SUMMARY

It is reasonable to suppose that TSQ compensation may permit to increase the luminosity in the case of zero dispersion at IP. To optimize the aspect ratio at a fixed detector field the use of a combined TSQ scheme is proposed.

6 REFERENCES

[1] D. Rubin et al, "CESR Beam-Beam Limit", PAC2001, Chicago, Illinois, June 2001.

[2] S.A. Nikitin & I.Ya. Protopopov, Preprint BINP 99-44, 1999.

[3] K. Steffen, Internal Report DESY HERA 82/11, 1982.

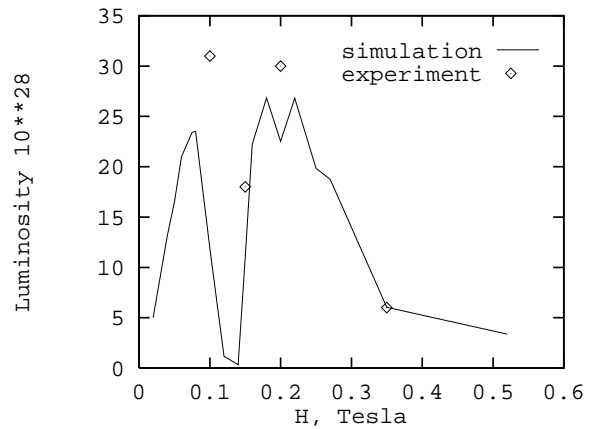[4] K. Hirata et al, "A Symplectis Beam-Beam Interaction with Energy Change", KEK Preprint 92-117, 1992.

Figure 8: Simulation (a solid line) and experimental (rhombs) dependences of the typical luminosity L_t upon the field H.